Antarctic Science 31(5), 271–285 (2019) © Antarctic Science Ltd 2019 doi:10.1017/S0954102019000270

Energy and water mass balance of Lake Untersee and its perennial ice cover, East Antarctica

BENOIT FAUCHER [1], DENIS LACELLE[1], DAVID A. FISHER[2], DALE T. ANDERSEN [3] and CHRISTOPHER P. McKAY [4]

[1]*Department of Geography, Environment and Geomatics, University of Ottawa, Ottawa, Canada*
[2]*Department of Earth and Environmental Sciences, University of Ottawa, Ottawa, Canada*
[3]*Carl Sagan Center, SETI Institute, Mountain View, CA, USA*
[4]*NASA Ames Research Center, Mountain View, CA, USA*
bfauc073@uottawa.ca

Abstract: Lake Untersee is one of the largest perennially ice-covered lakes in Dronning Maud Land. We investigated the energy and water mass balance of Lake Untersee to understand its state of equilibrium. The thickness of the ice cover is strongly correlated with sublimation rates; variations in sublimation rates across the ice cover are largely determined by wind-driven turbulent heat fluxes and the number of snow-covered days. Lake extent and water level have remained stable for the past 20 years, indicating that the water mass balance is in equilibrium. The lake is damned by the Anuchin Glacier and mass balance calculation suggest that subaqueous melting of terminus ice contributes 40–45% of the annual water budget; since there is no evidence of streams flowing into the lake, the lake must be connected to a groundwater system that contributes 55–60% in order to maintain the lake budget in balance. The groundwater likely flows at a rate of $\sim 8.8 \times 10^{-2}$ m^3 s^{-1}, a reasonable estimate given the range of subglacial water flux in the region. The fate of its well-sealed ice cover is likely tied to changes in wind regime, whereas changes in water budget are more closely linked to the response of surrounding glaciers to climate change.

Received 21 March 2019, accepted 18 June 2019

Key words: hydrology, ice-covered lake, sublimation

Introduction

Perennially ice-covered lakes are prominent features in ice-free, coastal Antarctica (Laybourn-Parry & Wadham 2014). Early investigations into the thermodynamics of ice-covered lakes in the McMurdo Dry Valleys (MDV) revealed that the thickness of the ice cover is primarily controlled by the balance between the conduction of energy out of the ice and the release of latent heat during freezing at the ice–water interface (Wilson *et al.* 1962, McKay *et al.* 1985). To maintain the energy balance in steady-state conditions, the rate of water freezing at the bottom of the ice cover must equal the ablation rate at the ice surface (sum of melting, evaporation and sublimation). It has been observed in the MDV lakes that ice cover and lake level respond rapidly to local variations in climate (Doran *et al.* 2008). In the MDVs, lake levels have risen several metres over the past two decades due to increased glacial meltwater inflow from ephemeral streams (e.g. Hawes *et al.* 2011, Castendyk *et al.* 2016), and lake ice thickness on the various lakes has waxed and waned (Clow *et al.* 1988, Doran *et al.* 2008, Dugan *et al.* 2013). The volume of meltwater received in the lakes was found to be proportional to the degree-days above freezing, and with predicted increase in summer warming, lake levels are predicted to continue to increase, thereby affecting ecological systems (Dugan *et al.* 2013, Gooseff *et al.* 2017).

In central Queen Maud Land, the Untersee Oasis contains two large perennially ice-covered lakes - Untersee and Obersee (Bormann & Fritzsche 1995, Schwab 1998). Lake Untersee has characteristics that differentiate it from the lakes in the MDV and elsewhere around the continent. Untersee is a closed-basin lake damned at the north end by the Anuchin Glacier, and it resides in a region with a climate dominated by intense sublimation. Interestingly, Untersee does not develop a moat during the summer when air temperatures rise above freezing, and there is little evidence of surface streams flowing into the lake (Andersen *et al.* 2015). It has been suggested that Lake Untersee is recharged from melting of the Anuchin Glacier (Hermichen *et al.* 1985, Wand *et al.* 1997). Thus far, studies of Untersee have focused primarily on physical and chemical limnology (Hermichen *et al.* 1985, Wand *et al.* 1997, 2006, Steel *et al.* 2015, Bevington *et al.* 2018) and microbial ecology (Wand *et al.* 2006, Andersen *et al.* 2011, Koo *et al.* 2017). Detailed studies have yet to investigate the thermodynamics of the ice cover and the hydrological balance of the lake. The objective of this study is therefore to investigate the energy and water mass balance of Lake Untersee and its ice cover in order to

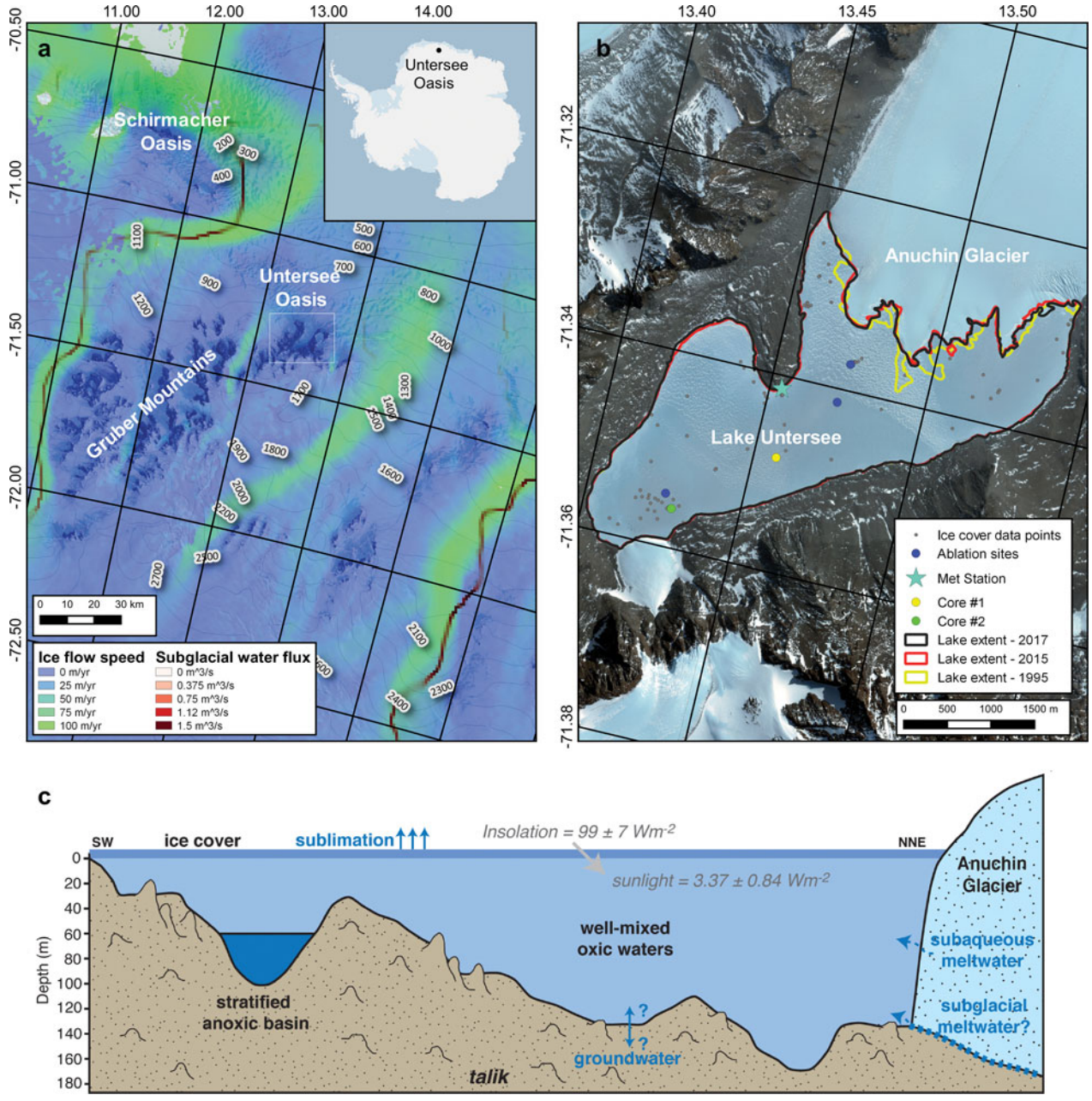

Fig. 1. Maps and cross-section showing: **a.** the location of the Untersee Oasis, adjacent regional ice-stream velocities (from Rignot *et al.* 2017) and regional subglacial water fluxes (from Le Brocq *et al.* 2013), **b.** location of ice-cover data sampling points (i.e. thickness, density), ablation measurement sites and ice cores on Lake Untersee's ice cover, and **c.** Lake Untersee's bathymetry, ice-cover solar radiation transmissivity and proposed input and output sources.

understand its current equilibrium and how it may evolve under changing climate conditions. This objective was achieved by determining: 1) the ice thickness and density across the lake; 2) the ablation and freezing rates of the ice; and 3) the contemporary changes in lake level and the relative contribution of inflows and outflows of water to the lake water balance. Based on the results, we assess the energy balance of Lake Untersee and its ice cover and discuss its fate under changing climate.

Study area

The Untersee Oasis is located in the Gruber Mountains of central Dronning Maud Land, *c.* 90 km south-east of the Schirmacher Oasis (Fig. 1). Elevations in the oasis range from 600 to 2790 m and local geology consists of norite, anorthosite and anorthosite–norite alternations of the Eliseev anorthosite massif (Bormann *et al.* 1986). The oasis was glaciated during the late Pleistocene and

https://doi.org/10.1017/S0954102019000270 Published online by Cambridge University Press

Table I. Inter-annual summer comparison of climatic data in the Untersee Oasis during the 2008–2018 period.

Summer	Average Dec/Jan/Feb temperature (°C)	Maximum Dec/Jan/Feb temperature (°C)	Minimum Dec/Jan/Feb temperature (°C)	Summer thawing index (degree-days)	Light (W m^{-2})
2008/09	-3.5	+5.3	-13.8	9.7	55.4[a]
2009/10	-1.9	+7.6	-12.8	37.7	99.3
2010/11	-2.2	+5.7	-12.9	22.4	99.9
2011/12	-3.6[b]	+4.4	-13.5	7.0	98.8
2012/13	-1.9[b]	+9.0	-12.1	51.3[c]	98.6
2013/14	-3.0	+10.6[d]	-11.1	16.3	94.6
2014/15	-3.2	+6.3	-13.4	8.1	99.7
2015/16	-3.0	+3.9	-10.3	11.5	98.0
2016/17	-1.9	+6.6	-13.9	29.7	n/a[e]
2017/18[f]	-2.3	+8.4	-12.8	32.6	n/a[e]

[a]Starting after 8 Dec 2008.
[b]Correct here (cf. Andersen *et al.* 2015 incorrect in table 1, correct monthly averages in table 2).
[c]48.8 degree-days excluding Nov 2012 (cf. Andersen *et al.* 2015).
[d]High temperatures corrected for loss of solar shield (11 Sep 2013–9 Dec 2014).
[e]Not available due to winter battery failure.
[f]Data from Data Garrison Station.

continues to receive ice flowing from a local ice field (elevation of *c.* 800 m) that is connected to the East Antarctic ice sheet (Schwab 1998). NASA's *MEaSUREs Annual Antarctic Ice Velocity Maps* (2011–2017) indicate that the Anuchin Glacier flows at an average velocity of *c.* 8–9 m yr^{-1}, with nearby ice streams to the east and west of Untersee Oasis flowing at an average velocity of *c.* 70–100 m yr^{-1} (Rignot *et al.* 2017; Fig. 1). In addition to Lakes Untersee and Obersee, numerous small ice-covered ponds reside on the western and eastern lateral moraines of the Anuchin Glacier. Schwab (1998) suggested that Lake Untersee likely formed between 12 and 10 kyr BP when the Anuchin Glacier retreated to near its present location.

Lake Untersee is located in a closed basin at *c.* 610 m a.s.l. and is dammed at its northern end by the Anuchin Glacier where a pressure ridge forms at the lake–glacier interface (Fig. 1). The lake is 2.5 km wide and 6.5 km long, making it the largest freshwater lake in central Queen Maud Land (Hermichen *et al.* 1985). With the exception of a boulder field at the south end of the lake and other large boulders scattered across the lake, the surface of ice cover on Lake Untersee is smooth and free of any fine sediments. The lake has two sub-basins: 1) a large basin occupies the northern and central section to a maximum depth of 169 m, and 2) a shallower basin occupies its southern section to depth of 100 m. The two basins are separated by a sill that cuts across the lake at 50 m depth (Wand *et al.* 1997). The water in the larger and deeper basin and above the sill in the shallower basin is well mixed and has a temperature near 0.5°C, pH near 10.6, dissolved oxygen near 150% and specific conductivity near 505 µS cm^{-1} (Wand *et al.* 1997, 2006, Andersen *et al.* 2011). The presence of the ice wall at the lake–glacier interface results in buoyancy-driven convection, allowing effective mixing throughout most of the lake with timescales of 1 month (Steel *et al.* 2015). However, in the southern basin, the water below the sill (60–100 m) is stratified, with temperatures ranging between 3°C and 5°C, lower pH (*c.* 7), higher specific conductivity (1100–1300 µS cm^{-1}) and dissolved oxygen levels near 0%. This anoxic water does not mix with the overlying oxic water due to its higher density (Bevington *et al.* 2018). The floor of the oxic sub-basin in Lake Untersee is covered by photosynthetic microbial mats, with the transparency of the lake ice to photosynthetically active radiation (PAR) being 4.9 ± 0.9% (Andersen *et al.* 2011).

The climate in the Untersee Oasis is part of a polar desert regime. Ten years of climate data (2008–2017) collected by an automated weather station along the shore of Lake Untersee (71.34°S, 13.45°E, 612 m a.s.l.) shows a mean insolation of 99 ± 7 W m^{-2}, mean annual air temperature (MAAT) of -9.5 ± 0.7°C, thawing degree-days ranging from 7 to 51 degree-days and a mean relative humidity of 42 ± 5% (Table I). The MAAT showed little to no change over the past decade (Table I). The average wind speed was 5.4 m s^{-1}, with a strong south wind descending from the polar plateau and sweeping across the southern section of the lake and also a strong east wind descending from the Aurkjosen Cirque and flowing across the snout of the Anuchin Glacier. Despite having a relatively warm MAAT for Antarctica, the climate in the oasis is dominated by intense ablation, which limits surface melt features due to cooling associated with latent heat of sublimation (e.g. Hoffman *et al.* 2008).

https://doi.org/10.1017/S0954102019000270 Published online by Cambridge University Press

Methodologies

Ice thickness and density of ice cover

During each expedition to Lake Untersee since 2008, holes were drilled through the ice cover using a 10 inch Jiffy drill. The ice thickness and freeboard (difference between height of the surface of the ice and water in the borehole) was determined using a 4 m pole graduated at 1 cm. From these two measurements, the density of the ice cover (in kg m^{-3}) was calculated from:

$$\rho_{ice} = \left(1 - \frac{Fb_i}{H_i}\right) \times 1000 \quad (1)$$

where Fb_i = freeboard (in cm) and H_i = thickness of ice cover (in cm).

Given the dimension of the lake, the locations of most drill holes were randomly selected, with one repeat location to verify ice thickness changes over time. The location of each drill hole ($n = 84$) was recorded with a handheld Garmin GPSMAP 64s GPS with accuracy of ± 3 m and the ice thickness and density data were added as points to ArcMap. The values were interpolated with ordinary spherical kriging where parameters (number of lags: 12 points; sector type: 8 sectors; maximum and minimum neighbours: 5 and 2) were set to obtain the lowest root-mean-square error. The interpolated results were displayed on a common scale and overlaid on a WorldView satellite image (acquisition date: 7 December 2015).

Ice cover ablation rates

Wand *et al.* (1996) reported the first ablation measurements at Lake Untersee based on measurement of three wooden ablation stakes in the ice cover; each was 4.5 cm in diameter and 4 m long and covered with white reflective tape. They reported ablation of the ice over 12 days in February 1995 was by 1 cm at the north end of the lake, 3 cm at the south end of the lake and 2.5 cm midway. No detailed descriptions of the ablation stakes as observed the following year were published.

On 7 December 2008, we inserted ablation ropes (*c.* 10 m lengths of braided 5 mm diameter white polyester) into seven holes drilled through the ice on a north–south transect, similar to that used by Wand *et al.* (1996), as well as five holes in the north-east and north-west corners of the lake (Fig. 1). Holes were backfilled with snow and ice to ensure the lines froze into the 15 cm diameter drill holes. Three years later, we recovered some but not all of the ablation lines; extensive snow cover on the lake that year made the finding and recovery of the ropes difficult.

Ice cover freezing rates

An approach to quantifying the amount of ice freezing at the ice–water interface based on the properties of the ice in the ice cover has not yet been developed for perennially ice-covered lakes. The abundance of gas bubbles occluded in the ice cover should vary as freezing progresses and excess dissolved air develops in the water (Lipp *et al.* 1987, Killawee *et al.* 1998). The stable isotopes of water (δD-δ^{18}O) will also evolve during closed-system freezing, such as for the ice cover of Lake Untersee (i.e. Lacelle 2011). Given that freezing at the ice–water interface largely occurs in winters (i.e. Clow *et al.* 1988, Dugan *et al.* 2013), the bubble abundance and δD-δ^{18}O values in the ice cover should reflect seasonal freezing of the water.

To verify whether the bubble abundance and δD-δ^{18}O values in the ice cover preserve information related to freezing rates, the ice cover of Lake Untersee was sampled at its central and southern sectors in December 2017 (Fig. 1). The ice was sampled using a Cold Regions Research and Engineering Laboratory (CRREL) coring kit to a depth of *c.* 2 m to prevent mixing with lake water. The ice cores were first photographed in the field under a light table using a Nikon D850 camera (focal length of 35 mm and exposure time of 1/20 s). The ice cores were then sliced at 2 cm, allowed to melt in sealed Ziploc bags, transferred in high-density polyethylene bottles and shipped in coolers to the University of Ottawa, where they were stored at 4°C until analysis.

The distribution and morphology of air bubbles in the ice cover were extracted from the photographs of the ice cores using the *ImageJ* software. The photographs were first converted to 8-bit grayscale format and classified following thresholding as either: 1) area occupied by bubbles; or 2) bubble-free area. The size and distribution of the bubbles were extracted at 1 cm slices using the *analyze particles* tool (e.g. Kinnard *et al.* 2008).

The $^{18}O/^{16}O$ and D/H ratios were determined using a Los Gatos Research liquid water analyser coupled to a CTC liquid chromatography prep-and-load autosampler for simultaneous $^{18}O/^{16}O$ and D/H ratio measurements of H_2O and verified for spectral interference contamination. The results are presented using the δ-notation ($\delta^{18}O$ and δD), where δ represents the parts per thousand differences for $^{18}O/^{16}O$ or D/H in a sample with respect to Vienna Standard Mean Ocean Water (VSMOW). Analytical reproducibility values for $\delta^{18}O$ and δD were ± 0.3‰ and ± 1‰, respectively. Deuterium excess (d) was then calculated using the following equation: $d = \delta D - 8\delta^{18}O$ (Dansgaard 1964).

The periodicity of bubble content (%) and the distribution of $\delta^{18}O$ values were extracted via spectral analysis (Fourier transformation) using *R* software's *Spectrum* tool (*Stats* built-in package). Significant-amplitude spectrum peaks indicate the periodicity of freezing events. The frequencies were converted to

https://doi.org/10.1017/S0954102019000270 Published online by Cambridge University Press

annual ice accretion using the following equation:

$$\text{Annual ice accretion} = \frac{1}{x} \times SI \quad (2)$$

where x = peak frequency and SI = sampling interval (here 2 cm) (Blackman & Tuckey 1958).

Water mass balance of Lake Untersee

Lake Untersee is a closed-basin lake dammed at its northern end by the Anuchin Glacier. As such, the water mass balance of the lake can be determined from:

$$\Delta S = P + I_s + I_e + I_g - O_s - O_g \quad (3)$$

where ΔS = change in the volume of water, P is total annual precipitation, I_s, I_e and I_g are the inflows of surface water, subaqueous melting of terminus ice (originating from the melting of the submerged Anuchin Glacier at the ice–lake water interface) and groundwater (subglacial meltwater or other sources), respectively, and O_s and O_g are the outflows of surface water and groundwater, respectively.

The volume of water in Lake Untersee was determined from the bathymetry map of Wand *et al.* (2006), which was digitized and georeferenced in the *ArcMap* software. The relations between lake surface elevation, surface area and water volume were also compiled from the digitized bathymetry map. Changes in lake surface area between 1995 and 2017 were then determined using the Geomaud 1995 air photographs, which were digitized and georeferenced in *ArcMap*, and with the use of 2015 and 2017 WorldView satellite images (acquisition dates: 7 December 2015, 7 December 2017; image resolution: 50 cm). The lake extents in 1995, 2015 and 2017 were traced in *ArcMap* (World Geodetic System 1984; Universal Transverse Mercator Zone 33S) and the surface area computed from the derived polygons.

The sealed nature of Lake Untersee is such that direct precipitation (P) is likely not contributing to its water mass balance. The contribution of subaqueous melting of terminus ice from the Anuchin Glacier (I_e) was determined from its average annual velocity, its cross-sectional area at the ice–water interface (which assumes the glacier is grounded at the lake bed) and changes in the position of the glacial ice tongues at the contact with the lake. The velocity of the Anuchin Glacier was obtained by tracking the displacement of a target on its surface over a 10 year period (2008–2017). The position of the target was recorded with a handheld Garmin GPSMAP 64s GPS with accuracy of ± 3 m. The target velocity data were compared to the 2011–2017 NASA MEaSUREs Antarctic ice velocity (Rignot *et al.* 2017). The outflow of surface water (O_s) was determined from our calculation of the amount of ice loss by ablation.

Results

Thickness and density of the ice cover

Ice thickness measurements taken at the same location between 2011 and 2017 provided near-identical results (3.78 ± 0.07 m; n = 4), indicating that measurements obtained over a 10 year period should have little effect on estimating ice thickness. The measurements of the ice cover thickness range from 1.96 to 3.96 m, with a bimodal distribution (median = 2.52 m; average = 2.76 ± 0.59 m; n = 89). Based on geostatistical kriging interpolation, the average lake ice thickness is 2.77 ± 0.25 m. Ice thickness shows a general north–south trend, with thicker ice cover in the north-west sector and thinner ice in the south and north-east sectors (Fig. 2). The density of the ice cover ranges from 764 to 1000 kg m^{-3}, with an average of 902 ± 47 kg m^{-3}. Geostatistical interpolation indicates an average ice density of 891 ± 5 kg m^{-3}. Under-dense ice (< 850 kg m^{-3}) is found in the central section of the lake, due east of the moraine, and over-dense ice (near 1000 kg m^{-3}) is found in the north-east sector.

Ablation rates from ablation ropes

On 17 November 2011, two ablation ropes at the southern end of the lake indicated net ablations of 230 and 213 cm over 3 years. On 18 December 2011, an additional 7 cm of ablation was measured. These results indicate annual average ablation rates of 78 and 72 cm yr^{-1} at the two sites. Three ablation ropes due east of the meteorological station (central area of the lake) indicated ablations of 116, 117 and 122 cm, corresponding to annual average ablation rates of 39, 41 and 39 cm yr^{-1}, respectively. From this, we infer that the yearly ablation rate is *c.* 40 ± 1.2 cm yr^{-1} in the central portion of the lake, and it increases to *c.* 75 ± 4.2 cm yr^{-1} at the southern end of the lake, where some of the thinnest ice is also observed.

Freezing rates from bubble morphology and δD-δ^{18}O composition of ice cover

The ice cover of Lake Untersee contains a range of bubble sizes and shapes (Fig. 3). In both ice cores, the shapes of the bubbles were either spherical, oval, dendritic or tubular. The ice cover in the central sector had a bubble content ranging from 2% to 50%, with higher bubble content and variability in the uppermost 75 cm (peak of 50% at 54 cm depth) (Fig. 4). Bubble content was more constant below 100 cm, where it varied between 2% and 18%. The ice cover in the southern sector had bubble contents ranging from 0.3% to 46%, with higher bubble contents in the uppermost 150 cm. No particular trend was observed for the bubble content, but three peaks were identified at depths of 18, 85 and 135 cm. The δ^{18}O

https://doi.org/10.1017/S0954102019000270 Published online by Cambridge University Press

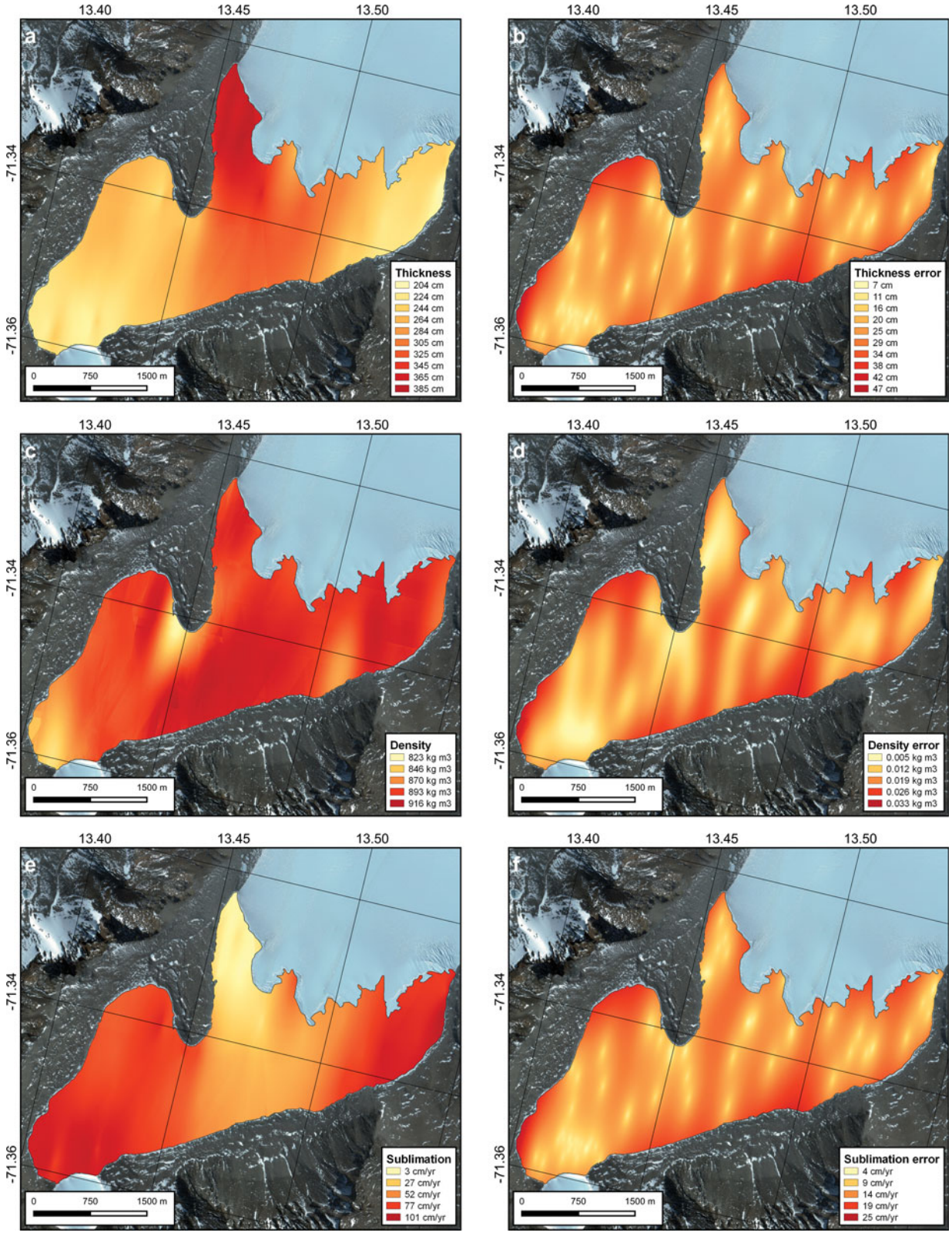

Fig. 2. WorldView images (7 December 2017) of Lake Untersee showing: **a.** interpolated ice-cover thickness, **b.** interpolated ice-cover thickness errors, **c.** interpolated ice-cover density, **d.** interpolated ice-cover density errors, **e.** interpolated annual ice-cover sublimation rate, and **f.** interpolated annual ice-cover sublimation rate errors.

https://doi.org/10.1017/S0954102019000270 Published online by Cambridge University Press

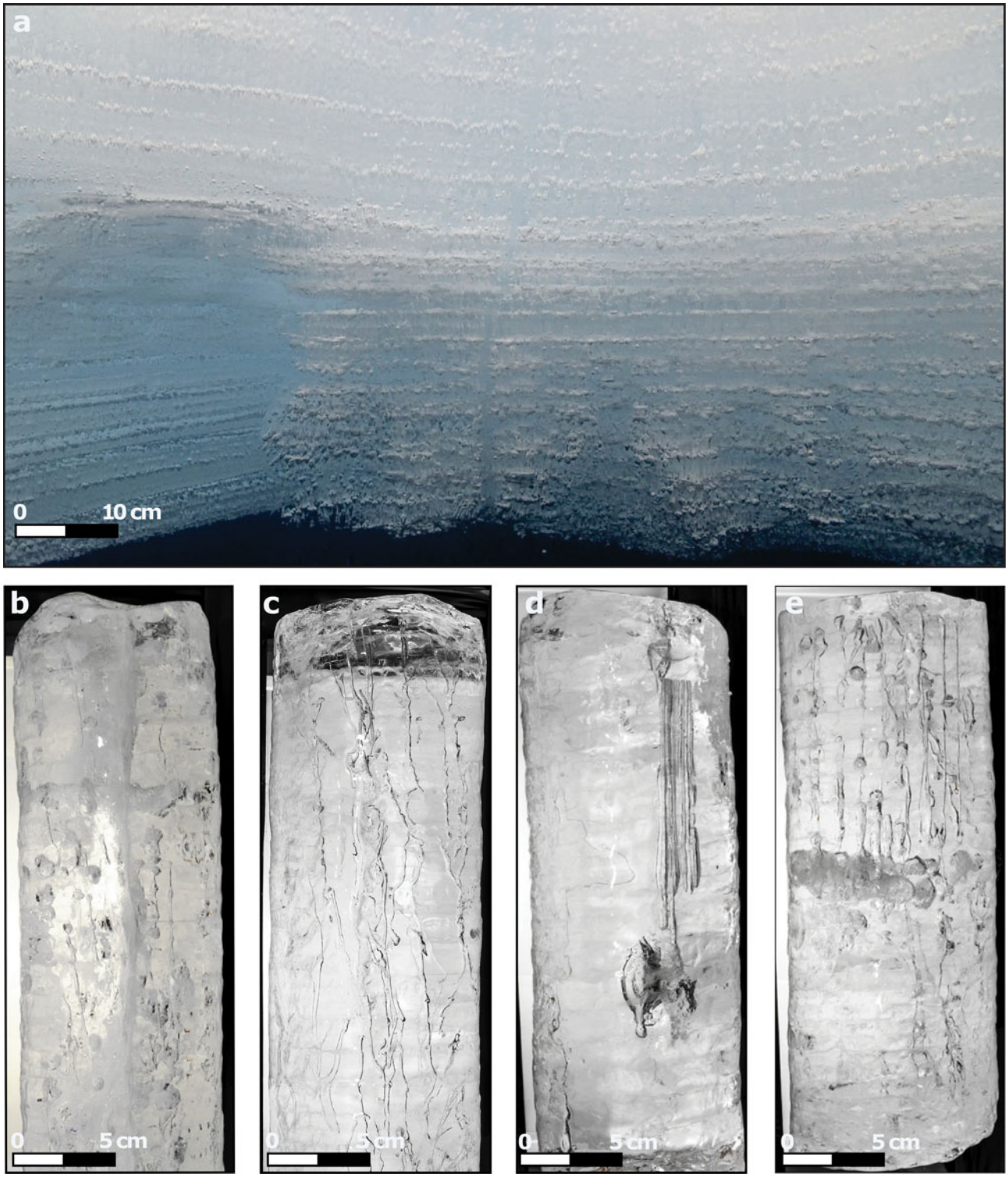

Fig. 3. Ice-cover bubble abundance and morphology. **a.** Underwater view of bubbles in the lower portion of the ice cover; **b.–e.** examples of different morphologies of bubbles observed in ice cover: **b.** spherical bubbles in core #1, **c.** dendritic bubbles in core #1, **d.** tubular and oval bubbles in core #2, and **e.** tubular and spherical bubbles in core #2.

values in the ice core from the central sector ranged from -35.5‰ to -34.2‰, whereas D-excess values ranged from -1.31‰ to 6.9‰. The $\delta^{18}O$ and D-excess values showed decreasing and increasing trends with depth, respectively. The $\delta^{18}O$ values in the southern sector ice fluctuated from -36.2‰ to -35.6‰, with D-excess varying from

https://doi.org/10.1017/S0954102019000270 Published online by Cambridge University Press

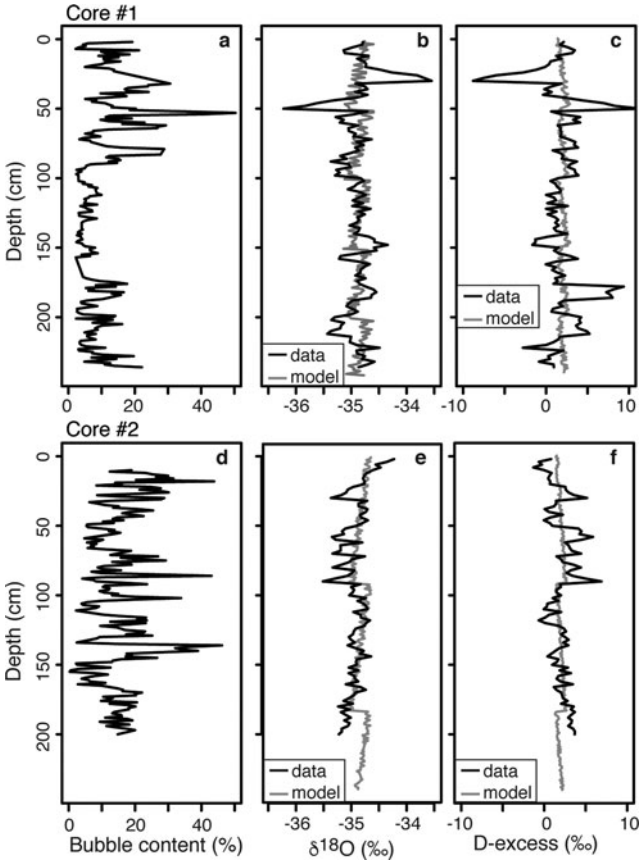

Fig. 4. Depth profiles of bubble content (%), $\delta^{18}O$ and D-excess measurements in **a.–c.** core #1, and **d.–f.** core #2. Modelled annual ice-cover coevolution of $\delta^{18}O$ ratios and D-excess is shown in grey.

-8.8‰ to 11.4‰. Variations in $\delta^{18}O$ and D-excess values were negatively correlated in the uppermost 50 cm; this was reflected to a lesser degree in the lower portion of the core, where $\delta^{18}O$ and D-excess values were much more stable.

The spectral power for the distribution of bubble abundance and $\delta^{18}O$ showed peaks at 0.041 and 0.022 for the core retrieved from the central and southern sectors of the lake, respectively (Fig. 5). The frequencies were converted to annual ice accretion ((1 / frequency) × 2 cm) and provided freezing rates of 49 cm yr^{-1} at the central section and 91 cm yr^{-1} at the southern section of the lake.

Water mass balance of Lake Untersee

Analysis of the bathymetry of Lake Untersee with the *Surface Volume* tool in *3D Analyst* (*ArcGIS 10* software) demonstrates that lake surface area and lake water level are positively correlated; it is only when the lake level is below 520 m that a further lowering of the water level results in small changes in surface area (Fig. 6). Based on the digitized bathymetry, Lake Untersee has a water volume of 5.21×10^8 m^{-3}. In 2017 and 2015, Lake Untersee had surface areas of 8.73 and 8.72 km^2, respectively, values that are slightly greater than what was measured in 1995 (8.45 km^2). The difference in surface area between 1995 and 2017 is caused by two of the Anuchin Glacier's ice tongues that retreated by 420 and 480 m, respectively. Visual comparison of oblique air photographs from 1939 also show little variation in the extent of Lake Untersee, which implies that its extent has been relatively stable for the past 80 years. The ice cover where the ice tongues had receded is composed of both lake ice and patches of white glacier ice that have been smoothly ablated to the same elevation as the lake ice (Fig. 1b). Unlike the lake ice that is sediment free, the patches of glacier ice in the ice cover contain cryoconite holes.

The amount of direct precipitation (P) and inflow of surface water (I_s) contributing to the water mass balance of Lake Untersee can be ignored because: 1) the lake does not develop a moat in summer and hence rainfall cannot directly contribute to lake water; 2) no ephemeral streams feeding into the lake were historically observed; and 3) any snow that falls on the ice cover quickly sublimates or is blown away. The volume of subaqueous melting of terminus ice (I_e) was estimated from the velocity of the Anuchin Glacier, its cross-sectional area along the ice–water interface and changes in the location of the glacial ice tongues. A target placed on the surface of the Anuchin Glacier moved 76 m at an azimuth of 183° between 2008 and 2017, which corresponds to a mean annual ice velocity of 8.4 m yr^{-1}, which is in the range reported by MEaSUREs annual Antarctic ice velocity (*c.* 8–9 m yr^{-1} on average between 2011 and 2017; Fig. 1). Based on the bathymetry along the lake–glacier interface and the width of the glacier along the lake, the cross-sectional area of the ice wall is estimated to be 0.27 km^2. Therefore, subaqueous melting of the Anuchin Glacier's terminus contributes annually $1.98–2.23 \times 10^6$ m^3 of water volume to the lake. The volume of surface water (O_s) loss was determined from our calculation of ablation of the ice cover, which ranges between *c.* 40 cm yr^{-1} in the central portion of the lake and increases to *c.* 75–80 cm yr^{-1} in the southern end of the lake. The range in rates of annual ablation translates into annual water loss in the order of $3.22–6.43 \times 10^6$ m^3 (0.6–1.2% of the lake's volume).

Discussion

Spatial variations in ice cover thickness and ablation/freezing rates

The ice cover of Lake Untersee is in steady state because its thickness at the same location did not change between 2011 and 2017 (3.78 ± 0.07 m; $n = 4$). This means that the freezing and ablation rates of the ice cover must be

https://doi.org/10.1017/S0954102019000270 Published online by Cambridge University Press

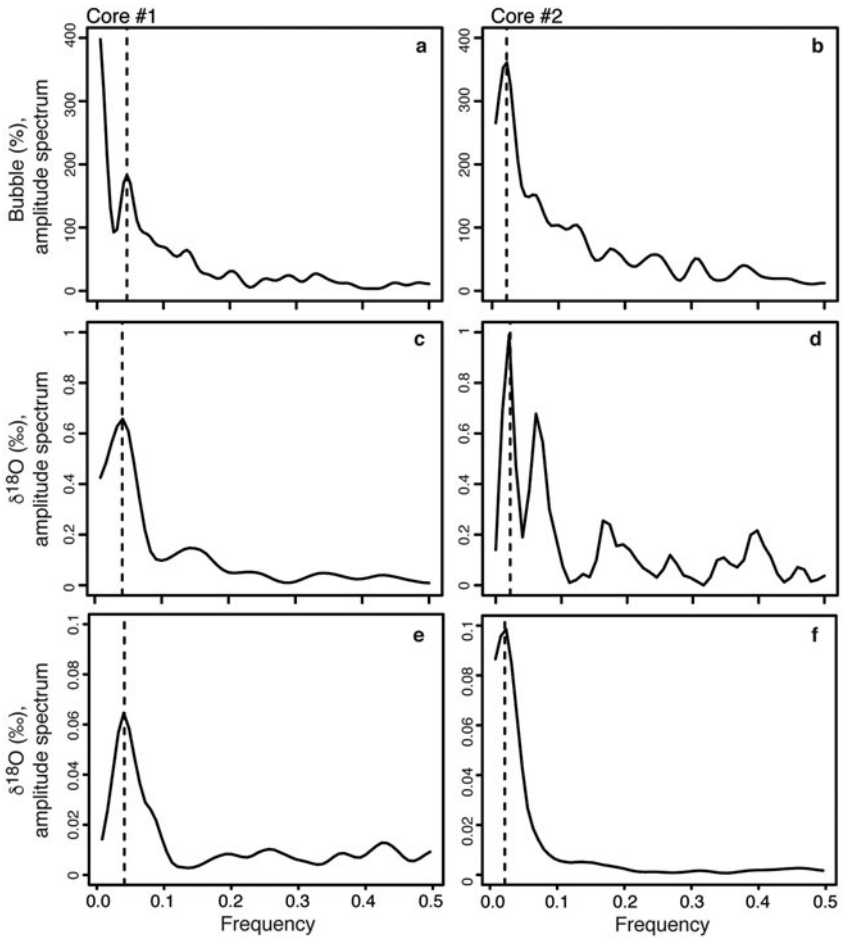

Fig. 5. Amplitude spectra in radians for $\delta^{18}O$ and bubble content (%) in (**a.** & **c.**) core #1, and (**b.** & **d.**) core #2. Frequencies can be converted to annual ice accretion ($1/X \times 2$), where X is the peak frequency. The dotted lines indicate the peak of the spectral signal frequencies for core #1 (*c.* 0.041 = 49 cm) and for core #2 (*c.* 0.022 = 91 cm). Amplitude spectra for modelled seasonal ice-cover freezing rates (using a simple Rayleigh-type fractionation of the residual water) of 49 cm (core #1) and 91 cm (core #2) are shown in **e.** and **f.**, respectively.

near equal (e.g. McKay *et al.* 1985). Our measurements from *in situ* ablation ropes provided ablation rates of *c.* 40 ± 1.2 cm yr^{-1} and *c.* 75 ± 4.2 cm yr^{-1} in the northern and southern sectors, respectively. The freezing rates derived from the frequency distribution of the bubbles and $\delta^{18}O$ vertical profiles in the ice cover yielded values of 49 ± 2 cm yr^{-1} in the central sector and 91 ± 2 cm yr^{-1} at the southern sector of the lake, similar to the nearby ablation rates.

Lipp *et al.* (1987) observed, although at a smaller scale, dendritic breakdown of the planar ice–water interface due to gas enrichment and bubbles nucleated in interdentritic spaces under closed-system freezing experiments of highly saturated gas solutions. Nucleation and growth of gas bubbles were seen to be periodic processes under certain circumstances, which was explained by the continuous build-up and reduction of the concentration of gases in the remaining solution. The δD-$\delta^{18}O$ measurements also allow for the determination of freezing events because in closed-system equilibrium freezing a progressive depletion in ^{18}O and D values in the residual water (and forming ice) occurs following Rayleigh-type fractionation (Lacelle 2001). In perennially ice-covered lakes, where repeated freezing occurs at the bottom of the ice cover, an isotopic discontinuity should separate the seasonal freezing events in the ice cover when the water column is well mixed, and this should be reflected in the $\delta^{18}O$ profile. The $\delta^{18}O$ composition of the ice cover during seasonal freezing was modelled using a simple Rayleigh-type fractionation of the residual water to assess whether the profile and the extracted frequency are similar to our measurements. The model assumes equilibrium freezing of 1% of the lake water (reflecting the amount of water that sublimates and that must freeze to maintain water balance) in 0.01% residual water fraction steps using the fractionation factors corrected for initial δD-$\delta^{18}O$ water composition (i.e. Jouzel & Souchez 1982) with an

https://doi.org/10.1017/S0954102019000270 Published online by Cambridge University Press

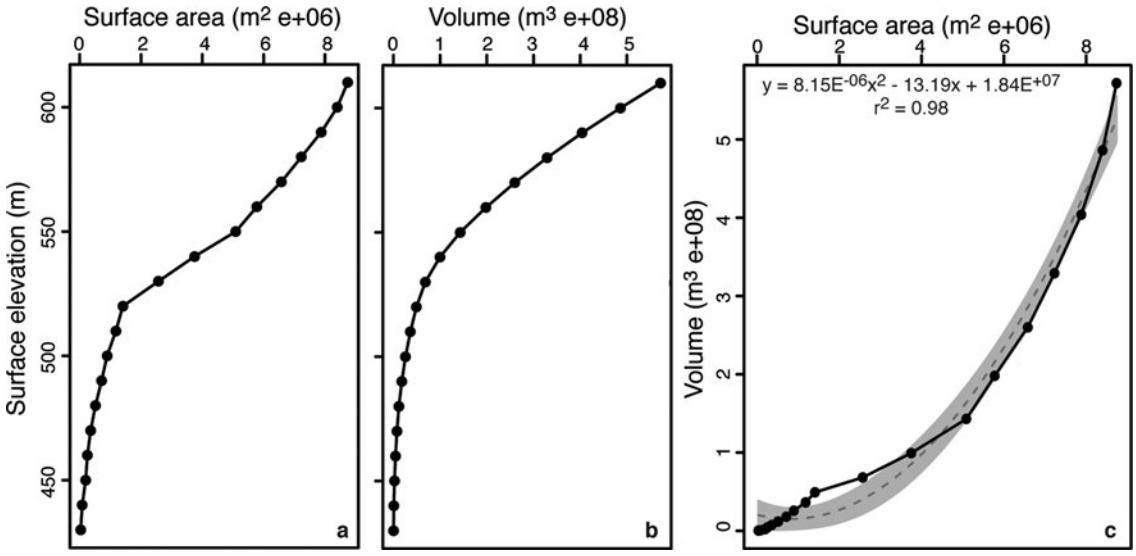

Fig. 6. Relation between lake surface elevation and **a.** surface area, and **b.** water volume. **c.** Relation between surface area and water volume. The dashed line is the best fit polynomial line. Analysis derived from bathymetry from Wand *et al.* (2006).

introduced noise signal of 100% variance and repeated for three to five freezing cycles. The modelled freezing thickness was adjusted to both coring sites (i.e. 49 and 91 cm yr^{-1}). The $\delta^{18}O$ composition of the ice cover matched well with the measured profile and spectral frequencies in both cores (Figs 4 & 5). The D-excess values obtained from this modelling also gave a good fit with the profile measurements. It thus appears that the frequency distribution of $\delta^{18}O$ and the bubble content in the ice cover preserves information about the thickness of annual freezing at the bottom of the ice cover.

The thickness of the ice cover of the 6.5 km long Lake Untersee shows a general north–south trend, with thicker ice cover in the north-west sector (*c.* 3.50–3.96 ± 0.10 m) and thinner ice in the south and north-east sectors (*c.* 1.96–2.50 ± 0.10 m). The ice cover is thinner than most of the ice-covered lakes in the MDV, where they range from 3 to 6 m, despite considerable variations in depth, temperature and salinity between the lakes (Doran *et al.* 2002). A significant negative relation exists between the ice thickness and ablation/freezing rates (Fig. 7). The relation was used to derive the ablation rate across the entire lake using geostatistical interpolation, which averaged 61 ± 13 cm yr^{-1} (median = 68 cm yr^{-1}). Like the systematic increase in ice thickness from north to south in the lake, the ablation rates increase along this same direction; this suggest that ablation has a strong controlling effect on ice thickness. Considering the little change over the past decade in insolation, MAAT, thawing degree-days and relative humidity (Table I), the spatial variation in ablation rates across the ice cover is likely due to the persistent strong south winds descending from the Sjobotnen Cirque and sweeping across the

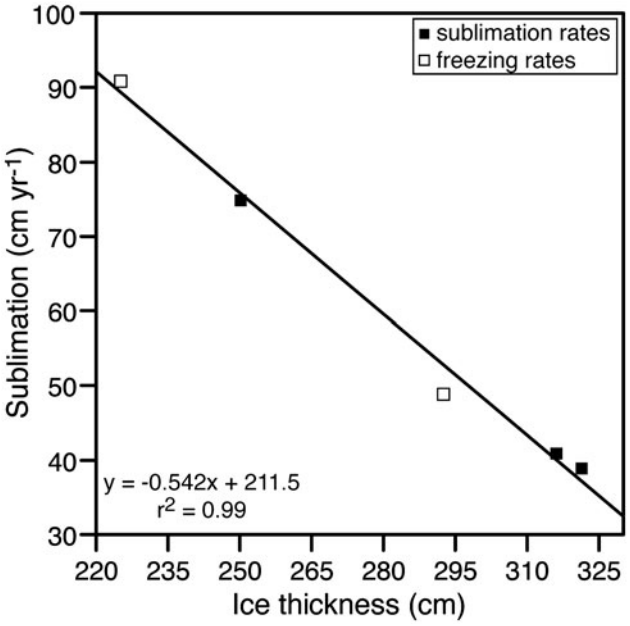

Fig. 7. Relation between the ice-cover thickness and ablation/freezing rates. White and black squares indicate freezing rates inferred from spectral analysis of ice-cover cores and measured ice-cover sublimation rates, respectively.

southern section of the lake (average wind speed of 4.9 m s^{-1} in summer 2011) and also the strong east wind descending from the Aurkjosen Cirque (average wind speed of 6.2 m s^{-1} in summer 2011) and flowing across the snout of the Anuchin Glacier. The central area of the lake where the thicker ice is found is sheltered from the strong winds (average wind speed of 4.2 m s^{-1} in summer 2011), as evidence of the snow-shadow on the lake ice (Fig. 1b).

https://doi.org/10.1017/S0954102019000270 Published online by Cambridge University Press

Heat energy model of the ice cover

Clow *et al.* (1988) developed a climate-based model that incorporated non-steady molecular diffusion into Kolmogorov-scale eddies to derive the average sublimation rate of the ice cover of lakes in the MDV (*c.* 30 cm yr^{-1}). Given that the MAAT at Lake Untersee is *c.* 7°C warmer than that used by Clow *et al.* (1988), the sublimation rate of the ice cover of Lake Untersee is expected to be *c.* 1.8× higher, a factor given by the ratio of the vapour pressure of ice at -9.5°C and -17.0°C. This first-order scaling would predict an average sublimation rate at Lake Untersee of 60 cm yr^{-1}, similar to the average ablation rate of 61 ± 13 cm yr^{-1}. However, the thickness of the ice cover of Lake Untersee has a strong spatial variation that appears to be associated with the wind regime across the lake. To test for the effect of wind on sublimation rates, we assume that the energy required to sublimate the ice comes from turbulent heat flux caused by the wind blowing over the ice surface (i.e. Paterson 2010). We used a standard turbulent heat flux equation for smooth-surface ice to calculate the thickness of ice that can sublimate annually from variable wind speeds (*SR*, in m yr^{-1}) using:

$$SR = \frac{22.2\ A\ u\ (e_s - e)t}{L_v \rho_{ice}} \quad (4)$$

where $A = 0.002$ (the transfer coefficient for air moving over smooth ice with temperatures in the -10°C to 0°C range; Ambach & Kirchlechner 1986), u is the wind speed (m s^{-1}) at screen height (1 m), e_s is the saturation water vapour pressure over ice (at the ice surface temperature in Pa; a value that is *c.* 600 Pa for ice near 0°C) and e is the water vapour pressure at screen height (relative humidity = 42%, so $e \approx 252$ Pa), t is the number of seconds in a year (3.153×10^7), L_v is latent heat of vaporization (3.1335×10^6 J kg^{-1}) and ρ_{ice} is the density of ice (917 kg m^{-3}).

The theoretical amount of sublimating ice as a result of turbulent heat flux shows a linear relation with wind speed blowing over the ice surface (Fig. 8). Our measured summer 2011 average wind speeds and sublimation rates show good fit with the theoretical line. The locations on the lake with slightly lower sublimation rates than predicted is attributed to the presence of snow on the ice surface, which would decrease the time during which sublimation is occurring (i.e. it would reduce the value of t in Eq. (4) to < 1 year). Therefore, variations in sublimation rates on the ice cover appears to be largely influenced by wind and associated with its turbulent heat flux and the number of snow-covered days (which reduce the sublimation of the ice cover).

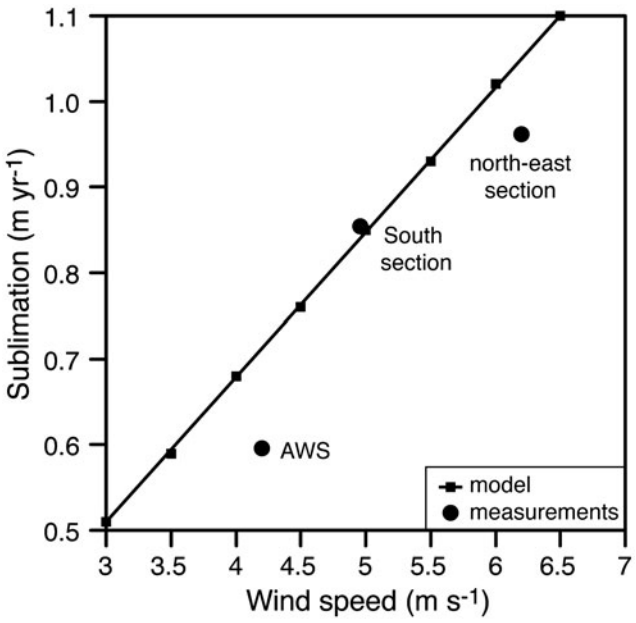

Fig. 8. Relation between wind speeds and sublimation rates at three locations on the ice cover. See Fig. 1 for the locations of the sites.

Water mass balance and heat energy model of Lake Untersee

Lake Untersee has a water volume of 5.21×10^8 m^{-3} and has remained stable since at least 1995 and was most likely stable for the past 80 years. With a surface area of 8.73 km^2 and an average sublimation rate of 61 ± 13 cm yr^{-1}, Lake Untersee is losing annually $4.90 \pm 1.03 \times 10^6$ m^3 of water (0.94 ± 0.20% of total lake water volume). Assuming that sublimation from the ice cover is the only output of water for the lake, then the lake must receive an equal inflow to maintain the water budget in equilibrium. There are no visible inflows of surface water to the lake, and direct precipitation does not contribute to the lake water. Hermichen *et al.* (1985) inferred that the lake was being recharged by melting of the Anuchin Glacier with no distinction between subaqueous melting of terminus ice and subglacial meltwater or other potential groundwater sources. The Anuchin Glacier advances towards Lake Untersee at a velocity of 8–9 m yr^{-1}, and since the ice tongues at the glacier–lake interface have remained at the same location for at least the past 30 years, subaqueous melting of terminus ice contributes $1.98–2.42 \times 10^6$ m^3 to the lake annually (40–45% of annual lake water volume; Fig. 9a). Therefore, *c.* $2.68–2.92 \times 10^6$ m^3 (55–60% of annual lake water volume) must be contributed annually from subglacial meltwater and/or a distinct groundwater source. This equates to a discharge of *c.* 8.8×10^{-2} m^3 s^{-1}, a reasonable flux given the reported range of subglacial water flux in the region (Fig. 1a). Therefore, Lake

https://doi.org/10.1017/S0954102019000270 Published online by Cambridge University Press

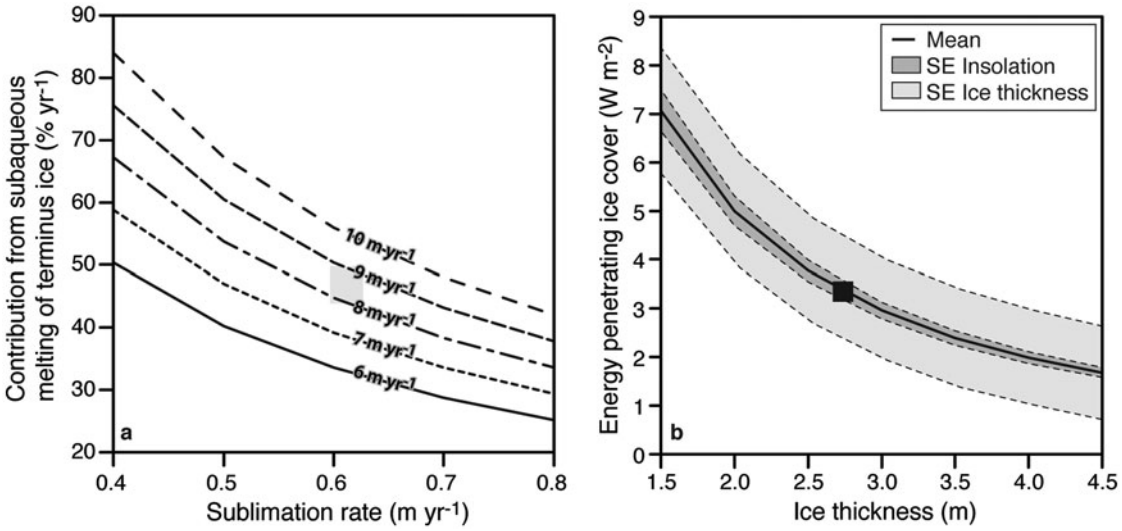

Fig. 9. a. Annual contribution of subaqueous melting of terminus ice to Lake Untersee as a function of various ice-cover sublimation rates and glacial velocities. **b.** Transmissivity of the ice cover to visible light (based on photosynthetically active radiation measurements) as a function of ice thickness. SE = standard error.

Untersee must be hydrologically connected to a regional groundwater system, similar to what has been inferred for Lake Bonney in the MDV from airborne transient electromagnetic sensors (i.e. Mikucki *et al.* 2015).

Unlike the lakes in the MDV, there are no visible surface inflows of water to the lake that would bring sensible heat energy to the lake water. Therefore, the subaqueous melting of terminus ice must be accomplished by sunlight energy that penetrates the ice cover. To test whether there is enough sunlight that reaches the water column to melt annually 1.98–2.23 × 10^6 m^3 of the terminus of the Anuchin Glacier, we undertook an energy mass balance calculation. Previous studies (e.g. McKay *et al.* 1985, Palmisano & Simmons 1987) have used a simple Beer's Law, exp(-z/H), to estimate ice cover light penetration and fitted scale height (H) to PAR measurements (where z is the ice cover thickness). This is incorrect in two ways: 1) in ice cover, scattering dominates over absorption and Beer's Law is for absorption only, and 2) the properties of the ice are not uniform over the PAR measurements. Here we use a simple scattering model for the lake ice cover that: 1) assumes uniform optical properties with depth, consistent with observations (absorption by very clean ice and scattering by large bubbles) (Fig. 3); 2) uses the absorption coefficient in ice as a function of wavelength from the latest compilation (i.e. Warren & Brandt 2008); and 3) uses a two-stream scattering model that includes absorption (i.e. eqs (3)–(7) in Sagan & Pollack 1967). There are two key parameters to this model: the total scattering optical depth and the scattering asymmetry factor. Given that ice is transparent mainly to the visible portion of the spectrum, a wavelength-resolved analysis was performed from 350 to 850 nm, which treated 850–3200 nm as a completely absorbing black body. Using our two measurements beneath the ice cover (PAR albedo = 0.66 and transmittivity = 0.049; Andersen *et al.* 2011) and assuming isotropic scattering by the bubbles in the ice cover to derive a fit to PAR measurements, we obtain a scattering optical depth of 9 m. The comparison to PAR measurements is determined by the average of 400–700 nm, weighted by the relative photon flux at each wavelength.

The flux of sunlight that penetrates the ice cover is determined by summing the computed solar flux transmissivity from 350 to 850 nm and the measured surface radiation (99 ± 0.7 W m^{-2}) from Andersen *et al.* (2015). Averaging over the range of the thickness of the ice cover (1.96–3.96 m), the energy reaching the water column is 3.37 ± 0.84 W m^{-2}; an amount that is sensitive to ice thickness (Fig. 9b). Neglecting loses of energy to the sides or bottom of the lake, which are expected to be minor, the mass of ice melted at the glacier–lake water interface is directly related to the solar energy entering the water column and can be calculated from:

$$Ice\_melt = (SoAt/L)/\rho_{ice} \quad (5)$$

where *Ice_melt* is the annual volume of ice melted (m^3 yr^{-1}), *So* is the solar flux entering the water column (W m^{-2}), A is the area of the lake (m^2), t is time in seconds, L is the latent heat of fusion of ice (J kg^{-1}) and ρ_{ice} is the density of ice.

According to Eq. (5), the 3.37 ± 0.84 W m^{-2} solar flux that enters the water column can melt 2.79 × 10^6 m^3 yr^{-1}, which is enough to sustain the annual contribution of the subaqueous melting of terminus ice (1.98–2.23 × 10^6 m^3).

https://doi.org/10.1017/S0954102019000270 Published online by Cambridge University Press

Considering that the annual contribution of subaqueous melting of terminus ice is dependent on the velocity of the Anuchin Glacier, there would be enough sunlight energy entering the water column to sustain subaqueous melting for contributions of up to 54%, an equivalent in glacier velocity of up to 11.4 m yr^{-1}.

Lake Untersee and changing climate

Lakes are good indicators of climate change because of their physical, chemical and biological responsivity to changes in environmental conditions (Williamson *et al.* 2009). Ten year measurements of ice-cover thickness of Lake Untersee showed little change; this is in contrast to lakes in the MDV that decreased by over 2 m between 1999 and 2016 (Obryk *et al.* 2019). The Untersee Oasis has a relatively warm MAAT for Antarctica; in fact, it is *c.* 7°C warmer than in the coastal zone in the MDV (i.e. Clow *et al.* 1988, Doran *et al.* 2002). Our climate measurements indicate that the MAAT in the Untersee Oasis has been relatively stable during the past decade (2008–2018; Table I). This is in contrast to the rest of the Queen Maud Land region, where MAAT has increased at a rate of 1.1 ± 0.7°C per decade between 1998 and 2016 (Medley *et al.* 2018), and with the MDV, where air temperature has increased since 2006 with no distinct trend (Obryk *et al.* 2019). Compared to the MDV ice-covered lakes, Lake Untersee should be developing a moat in summer, given the similar range in thawing degree-days (7–51) and higher MAAT; however, no moat develops around Lake Untersee, even during summers with a high number of thawing degree-days. A minor increase in summer air temperature is not expected to alter this condition, as the region is dominated by intense sublimation, which limits surface melt features and prevents summer moats from developing around the edges of the lake due to the cooling associated with the latent heat of sublimation (e.g. Hoffman *et al.* 2008). However, a change in wind regime should have a significant impact on the lake ice dynamic as it largely drives the sublimation and controls the thickness of the ice cover and consequently the proportion of solar radiation that enters the water column.

A more direct impact of climate change on the hydrology of Lake Untersee would be its effect on the surrounding glaciers, namely the Anuchin Glacier. Currently, the Anuchin Glacier has a velocity of 8–9 m yr^{-1}, and given that the position of the glacier–lake interface has not changed over the past 10 years, we assume that the amount by which the glacier advances all melts and contributes *c.* 40–45% of the annual lake water volume input. However, under the current ice cover thickness configuration, only *c.* 3.37 W m^{-2} of sunlight reaches the water column, which provides enough energy to melt a maximum of 2.79×10^{-3} km^3 of subaqueous ice along the ice wall. This volume would be exceeded if the velocity of the Anuchin Glacier exceeded 11.4 m yr^{-1}; in that case, lake water level would rise since the glacier would advance and act like a piston and force the water level to increase. On the other hand, a receding Anuchin Glacier would lower the water level by *c.* 9% of the receding distance (difference in density between ice and water, and the thickness of the glacier is approximately equal to the average depth of the lake). The responses of other potential water sources with regards to climate change are also uncertain. Currently, no surface streams are feeding into Lake Untersee; however, it is possible that, under a warming scenario, the lake would receive a contribution a surface runoff from ephemeral streams and supraglacial runoff. In that case, the lake would receive sensible and latent heat, which would drastically alter the hydrochemical conditions (i.e. allowing for interactions with the atmosphere) of the lake waters and may cause severe shifts in benthic biochemical regimes. If this happens, Lake Untersee would become more similar to lakes in the coastal MDV.

Conclusions

This study investigated the thermodynamics and the hydrological balance of Lake Untersee, one of the largest perennially ice-covered lakes in East Antarctica. Based on the results, the following conclusions can be drawn:

1. $\delta^{18}O$ and bubble content (%) trends in the ice cover can identify the annual thickness of ice accretion, and as such, when combined with ablation rate measurements, steady-state conditions of perennially ice-covered lakes can properly be determined.
2. Ten year measurements at the same location showed that the ice cover had near-identical thickness, indicating that the ice cover is in steady state.
3. The sublimation rate of Lake Untersee (and its control over ice-cover thickness) is largely influenced by wind (its associated turbulent heat flux) and the number of snow-covered days. With an annual average ablation rate of 61 ± 13 cm yr^{-1}, the ice cover has a turnover rate of 3–6 years.
4. Lake Untersee has a water volume of 5.21×10^8 m^{-3} and is losing annually 0.94 ± 0.20% of total lake water volume. The Anuchin Glacier advances towards Lake Untersee at a velocity of 8–9 m yr^{-1}, and subaqueous melting of terminus ice contributes 40–45% of annual lake water volume; the remaining volume must be contributed annually from subglacial meltwater and/or a groundwater source likely flowing at a rate of *c.* 8.8×10^{-2} m^3 s^{-1} into Lake Untersee. This provides one of the first - albeit indirect - pieces

https://doi.org/10.1017/S0954102019000270 Published online by Cambridge University Press

of evidence of groundwater recharging lakes in an ice-free region of Antarctica.

5. Based on a simple scattering model for the lake ice cover, 3.37 ± 0.84 W m^{-2} enters the water column. This provides enough energy to melt the ice along the glacier–lake interface and would be sufficient to sustain melting up to a glacier velocity of 11.4 m yr^{-1}.

Acknowledgements

This work was supported by the TAWANI Foundation of Chicago, the Trottier Family Foundation, the Natural Sciences and Engineering Research Council of Canada (NSERC) Discovery Grant, Polar Knowledge Canada, NASA's Astrobiology Program and the Arctic and Antarctic Research Institute/Russian Antarctic Expedition. A NSERC Alexander Graham Bell Canada Graduate Scholarship (doctoral) provided financial support to B. Faucher. Logistical support was provided by the Antarctic Logistics Centre International (ALCI), Cape Town, South Africa. We are grateful to Colonel (IL) J.N. Pritzker, IL ARNG (retired), of the TAWANI Foundation, Lorne Trottier of the Trottier Family Foundation and fellow field team members for their support during the expedition. We thank the two reviewers for their constructive comments.

Author contributions

Benoit Faucher: paper writing (main contributor); data collection; data analysis and interpretation; editing prior to paper's submission.

Denis Lacelle: paper writing; data collection; data analysis and interpretation; editing prior to paper's submission.

David A. Fisher: data analysis and interpretation; editing prior to paper's submission.

Dale T. Andersen: data collection; data analysis and interpretation; editing prior to paper's submission.

Christopher P. McKay: data collection; data analysis and interpretation; editing prior to paper's submission.

Supplemental data

Datasets are available in the supplementary online material (SOM); SOM 1: 2008–2017 target displacement on Anuchin Glacier; SOM 2: 2008–2018 ice thickness and freeboard measurements of ice cover.

A supplemental file will be found at https://doi.org/10.1017/S0954102019000270.

References

Ambach, W. & Kirchlechner, P. 1986. Nomographs for the determination of the meltwater from ice and snow surfaces by sensible and latent heat flux. *Wetter Leben*, **38**, 181–189.

Andersen, D.T., Sumner, D.Y., Hawes, I., Webster-Brown, J. & McKay, C.P. 2011. Discovery of large conical stromatolites in Lake Untersee, Antarctica. *Geobiology*, **9**, 280–293.

Andersen, D.T., McKay, C.P. & Lagun, V. 2015. Climate conditions at perennially ice-covered Lake Untersee, East Antarctica. *Journal of Applied Meteorology and Climatology*, **54**, 1393–1412.

Bevington, J., McKay, C.P., Davila, A., Hawes, I., Tanabe, Y. & Andersen, D.T. 2018. The thermal structure of the anoxic trough in Lake Untersee, Antarctica. *Antarctic Science*, **30**, 333–344.

Blackman, R.B. & Tukey, J.W. 1958. *The measurement of power spectra*. New York, NY: Dover Publications, 190 pp.

Bormann, P. & Fritzsche, P., *eds.* 1995. *The Schirmacher Oasis, Queen Maud Land, East Antarctica, and its surroundings*. Gotha, Germany: Justus Perthes Verlag, 448 pp.

Bormann, P., Bankwitz, P., Bankwitz, E., Damm, V., Hurtig, E., Kampf, H. *et al.* 1986. Structure and development of the passive continental margin across the Princess Astrid Coast, East Antarctica. *Journal of Geodynamics*, **6**, 347–373.

Castendyk, D.N., Obryk, M.K., Leidman, S.Z., Gooseff, M. & Hawes, I. 2016. Lake Vanda: a sentinel for climate change in the McMurdo Sound Region of Antarctica. *Global Planet Change*, **144**, 213–227.

Clow, G.D., McKay, C.P., Simmons Jr, G.M. & Wharton Jr, R.A. 1988. Climatological observations and predicted sublimation rates at Lake Hoare, Antarctica. *Journal of Climate*, **1**, 715–728.

Dansgaard, W. 1964. Stable isotopes in precipitation. *Tellus*, **16**, 436–468.

Doran, P.T., McKay, C.P., Clow, G.D., Dana, G.L., Fountain, A.G., Nylen, T., *et al.* 2002. Valley floor climate observations from the McMurdo Dry Valleys, Antarctica, 1986–2000. *Journal of Geophysical Research - Atmospheres*, **107**, 10.1029/2001JD002045.

Doran, P.T., McKay, C.P., Fountain, A.G., Nylen, T., McKnight, D.M., Jaros, C., *et al.* 2008. Hydrologic response to extreme warm and cold summers in the McMurdo Dry Valleys, East Antarctica. *Antarctic Science*, **20**, 499–509.

Dugan, H.A., Obryk, M.K. & Doran, P.T. 2013. Lake ice ablation rates from permanently ice-covered Antarctic lakes. *Journal of Glaciology*, **59**, 10.3189/2013JoG12J080.

Gooseff, M.N., Barrett, J.E., Adams, B.J., Doran, P.T., Fountain, A.G., Lyons, W.B., *et al.* 2017. Decadal ecosystem response to an anomalous melt season in a polar desert in Antarctica. *Ecology and Evolution*, **1**, 1334–1338.

Hawes, I., Sumner, D.Y., Andersen, D.T. & Mackey, T.J. 2011. Legacies of recent environmental change in the benthic communities of Lake Joyce, a perennially ice-covered Antarctic lake. *Geobiology*, **9**, 394–410.

Hermichen, D., Kowski, P. & Wand, U. 1985. Lake Untersee – the first isotope study of the largest fresh-water lake in the interior of East Antarctica. *Nature*, **315**, 131–133.

Hoffman, M.J., Fountain, A.G. & Liston, G.E. 2008. Surface energy balance and melt thresholds over 11 years at Taylor Glacier, Antarctica. *Journal of Geophysical Research*, **113**, 10.1029/2008JF001029.

Jouzel, J. & Souchez, R.A. 1982. Melting–refreezing at the glacier sole and the isotopic composition of the ice. *Journal of Glaciology*, **28**, 35–42.

Killawee, J.A., Fairchild, I.J., Tison, J.-L., Janssens, L. & Lorrain, R. 1998. Segregation of solutes and gases in experimental freezing of dilute solutions: implications for natural glacial systems. *Geochimica et Cosmochimica Acta*, **62**, 3637–3655.

Kinnard, C., Koerner, R.M., Zdanowicz, C.M., Fisher, D.A., Zheng, J., Sharp, M.J., *et al.* 2008. Stratigraphic analysis of an ice core from the Prince of Wales Icefield, Ellesmere Island, Arctic Canada, using digital image analysis: high-resolution density, past summer warmth reconstruction, and melt effect on ice core solid conductivity. *Journal of Geophysical Research*, **113**, 10.1029/2008JD011083.

Koo, H., Mojib, N., Hakim, J.A., Hawes, I., Tanabe, Y., Andersen, D.T., *et al.* 2017. Microbial communities and their predicted metabolic

functions in growth laminae of a unique large conical mat from Lake Untersee, East Antarctica. *Frontiers in Microbiology*, **8**, 1347.

Lacelle, D. 2011. On the $\delta^{18}O$, δD and D-excess relation in meteoric precipitation and during equilibrium freezing: theoretical approach and field examples. *Permafrost and Periglacial Processes*, **22**, 13–25.

Laybourn-Parry, J. & Wadham, J.L. 2014. *Antarctic lakes*. Oxford, UK: Oxford University Press.

Le Brocq, A.M., Ross, N., Griggs, J.A., Bingham, R.G., Corr, H.F.J., Ferraccioli, F., *et al*. 2013. Evidence from ice shelves for channelized meltwater flow beneath the Antarctic Ice Sheet. *Nature Geoscience*, **6**, 945–948.

Lipp, G., Korber, C., Englich, S., Hartmann, U. & Rau, G. 1987. Investigation of the behavior of dissolved gases during freezing. *Cryobiology*, **24**, 489–503.

McKay, C.P., Clow, G., Wharton Jr, R.A. & Squyres, S.W. 1985. Thickness of ice on perennially frozen lakes. *Nature*, **313**, 561–562.

Medley, B., McConnell, J.R., Neumann, T.A., Reijmer, C.H., Chellman, N., Sigl, M., *et al*. 2018. Temperature and snowfall in western Queen Maud Land increasing faster than climate model projections. *Geophysical Research Letters*, **45**, 1472–1480.

Mikucki, G., Auken, E., Tulaczyk, S., Virginia, R.A., Schamper, C., Sørensen, K.I., *et al*. 2015. Deep groundwater and potential subsurface habitats beneath an Antarctic Dry Valley. *Nature Communications*, **6**, 6831.

Obryk, M.K., Doran, P.T. & Priscu, J.C. 2019. Prediction of ice-free conditions for a perennially ice-covered Antarctic lake. *JGR Earth Surface*, **124**, 686–694.

Palmisano, A.C. & Simmons Jr, G.M. 1987. Spectral down-welling irradiance in an Antarctic lake. *Polar Biology*, **7**, 145–151.

Paterson, W.S.B. 2010. *The physics of glaciers, 4th ed*. Cambridge, MA: Academic Press, 721 pp.

Rignot, E., Mouginot, J. & Scheuchl, B. 2017. MEaSUREs InSAR-Based Antarctica Ice Velocity Map, Version 2. Boulder, CO: NASA National Snow and Ice Data Center Distributed Active Archive Center. Retrieved from http://dx.doi.org/10.5067/D7GK8F5J8M8R (accessed 15 February 2019).

Sagan, C. & Pollack, J.B. 1967. Anisotropic nonconservative scattering and the clouds of Venus. *Journal of Geophysical Research*, **72**, 469–477.

Schwab, M.J. 1998. Reconstruction of the late Quaternary climatic and environmental history of the Schirmacher Oasis and the Wohlthat Massif (East Antarctica). *Reports on Polar Research*, **293**, 1–128.

Steel, H.C.B., McKay, C.P. & Andersen, D.T. 2015. Modeling circulation and seasonal fluctuations in perennially ice-covered and ice-walled Lake Untersee, Antarctica. *Limnology and Oceanography*, **60**, 1139–1155.

Wand, U., Schwarz, G., Brüggemann, E. & Bräuer, K. 1997. Evidence for physical and chemical stratification in Lake Untersee (central Dronning Maud Land, East Antarctica). *Antarctic Science*, **9**, 43–45.

Wand, U., Samarkin, V.A., Nitzsche, H.-M. & Hubberten, H.-W. 2006. Biogeochemistry of methane in the permanently ice-covered Lake Untersee, central Dronning Maud Land, East Antarctica. *Limnology and Oceanography*, **51**, 1180–1194.

Warren, S.G. & Brandt, R.E. 2008. Optical constants of ice from the ultraviolet to the microwave: a revised compilation. *Journal of Geophysical Research - Atmospheres*, **113**(D14), 10.1029/2007JD009744.

Williamson, C.E., Saros, J.E., Vincent, W.F. & Smol, J.P. 2009. Lakes and reservoirs as sentinels, integrators, and regulators of climate change. *Limnology and Oceanography*, **54**, 2273–2282.

Wilson, A.T. & Wellman, H.W. 1962. Lake Vanda: an Antarctic lake: Lake Vanda as a solar energy trap. *Nature*, **196**, 1171–1173.